A PIEZOELECTRIC MICROVALVE WITH INTEGRATED SENSORS FOR CRYOGENIC APPLICATIONS

Jong M. Park[1], Tyler R. Brosten[2], Allan T. Evans[1], Kristian Rasmussen[2], Gregory F. Nellis[2], Sanford A. Klein[2], Jeffrey R. Feller[3], Louis Salerno[3], and Yogesh B. Gianchandani[1]
[1]Department of Electrical Engineering and Computer Science, University of Michigan, Ann Arbor
[2]Department of Mechanical Engineering, University of Wisconsin, Madison
[3]NASA Ames Research Center, Moffett Field, CA 94035

ABSTRACT

This paper describes a normally open, self-encapsulated, gas valve that has embedded sensors for pressure and temperature monitoring. The valve has been validated at operating temperatures over 80-380 K, and at pressures up to 130 kPa. A perimeter augmentation scheme for the valve seat has been implemented to provide higher flow modulation. Two kinds of suspensions are described for the valve seat. In tests performed at room temperature, the flow was modulated from 980 mL/min. with the valve fully open (0 V), to 0 mL/min. with 60 V actuation, at an inlet pressure of 55 kPa. Cryogenic flow rate tests show similar modulation with flow from 166 mL/min. with the valve fully open, to 5.3 mL/min. with 120 V actuation voltage, at an inlet pressure of 70 kPa. The platinum RTD temperature sensor is independently tested from 40-450 K with sensitivity of 0.23%/K in its operational range of 150-450 K. The pressure sensor has sensitivity of 250 ppm/kPa at room temperature.

I. INTRODUCTION

Cooling systems with a high degree of temperature stability and small gradients will be needed for systems such as optical assemblies or propellant depot stations for space missions. A distributed cooling network that uses multiple cooling elements can potentially meet these needs. Figure 1 illustrates how each cooling element can be realized: (a) a flow of cryogenic fluid at the load temperature through exchangers positioned across the structure to be cooled, or (b) a flow of cryogenic fluid at a higher temperature and pressure through recuperative heat exchanger, taking advantage of Joule-Thompson refrigeration. Either way, having valves that work reliably at cryogenic temperatures with large flow modulation capability is essential. This paper reports piezoelectric valves fabricated from Si, glass, and ceramic and their integration with temperature and pressure sensors. An early version of the basic valve was described in [1].

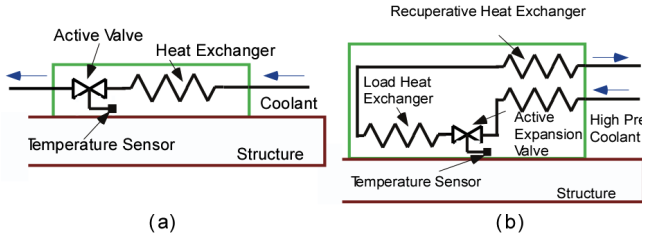

Fig. 1: Proposed application of actively controlled valve. Microvalves can (a) modulate flow of coolant in distributed heat exchangers, or (b) be used as expansion valves in Joule-Thompson cryocoolers.

II. DEVICE CONCEPTS AND OPERATION

The valve requires high forces across a wide temperature range to displace the Si against inlet pressure that can exceed 1 atm. Piezoelectric actuation is attractive because it can provide high forces, consumes negligible DC power and has acceptable cryogenic performance. Macor® (machinable glass ceramic) is chosen for the encapsulation material because of low thermal expansion at low temperature. In addition, it is machinable, capable of holding tight tolerances, exhibits no outgassing, and has zero porosity.

Out-of-plane, stacked PZT actuation has been widely used in valves [2-5]. However, as each valve is constructed for different applications, the performance goals are different. In our case, a normally open valve is desirable because the open condition is a safe failure mode, so that

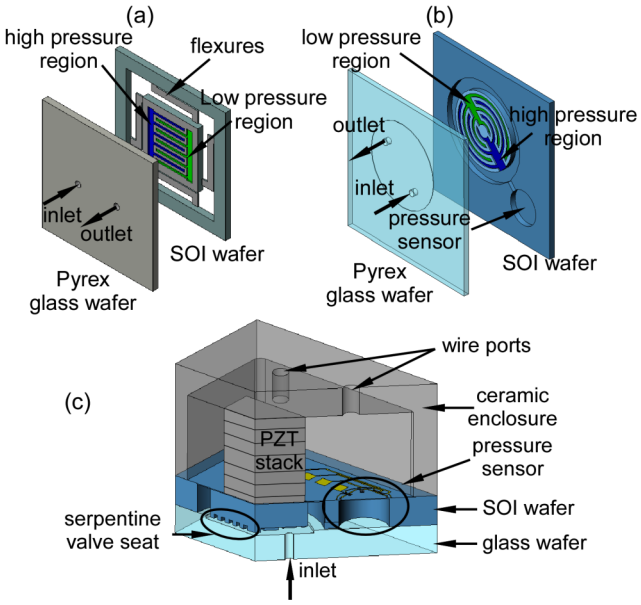

Fig. 2: Microvalve concepts: Two valve plate suspension types are described: (a) a valve plate suspended by flexures and (b) a valve plate suspended by membrane with integrated sensors. (c) A view of the membrane suspension ceramic-PZT-Si-glass structure cut away on the front and left sides.

flow of the refrigerant is not blocked. For the same reason, an extremely tight seal is not essential. Instead, this application requires valves working at cryogenic temperatures, able to withstand several atm. of inlet pressure, and able to provide large flow modulation (0-1000 mL/min).

The main challenge in using PZT actuation comes from small displacements that lead to modest flow modulation. This is addressed by using perimeter augmentation. The flow area for an out-of-plane valve (A_{valve}) is given by the product of the valve stroke (δ) and the perimeter of the valve seat (p).

$$A_{valve} = \delta \cdot p \qquad (1)$$

Thus, by increasing the perimeter of the valve seat, flow area can be increased substantially, which results in larger flow modulation. Extended serpentine grooves (127-160 mm in length) are fabricated on the valve plate as shown schematically in Fig. 2, to compensate for flow modulation. Each groove measures 50 μm wide and 120 μm deep. Two valve types with different valve seat suspensions are described here: a valve plate suspended by (a) flexures, and (b) a membrane.

Embedded temperature and pressure sensors enable closed loop control of a distributed cooling system. Temperature transduction devices are generally thermocouples or resistance-temperature-detectors (RTDs). The entire device is exposed to the operating temperature of the valve. This prevents the use of a thermocouple as the temperature sensor because of the difficulty in providing a reference. A platinum RTD was chosen because of its robustness and operating range (as low as 150K). A diaphragm pressure transduction method was chosen because of its ease of process integration. The two primary conversion mechanisms involve either capacitive or piezoresitive sensors. Piezoresistors were chosen because of their linearity and lower output impedance. These sensors are strategically placed in the membrane type valve to monitor the inlet gas pressure and temperature.

III. DEVICE FABRICATION

The fabrication process uses two wafers: a silicon-on-insulator (SOI) wafer which has a device layer, a buried oxide layer, and a carrier wafer thicknesses of 50 μm, 0.5 μm, and 450 μm, respectively, and a 500-μm-thick Pyrex glass wafer. The fabrication processes for SOI and glass wafers are illustrated in Fig. 3. A detailed fabrication process for flexure type valve is described in [1].

The use of the SOI wafer in the fabrication process permits the buried oxide layer to provide an etch stop for deep reactive ion etching (DRIE), while the epitaxial layer provides a well-controlled membrane thickness and bulk Si properties.

The top device layer side of the SOI wafer is implanted with a dopant and surface micromachined to create the pressure and temperature sensors. A 100-nm-thick platinum layer is used for the RTD. Then, the bottom side is patterned with Al and photoresist. The photoresist pattern acts as an etch mask for a DRIE step that is approximately

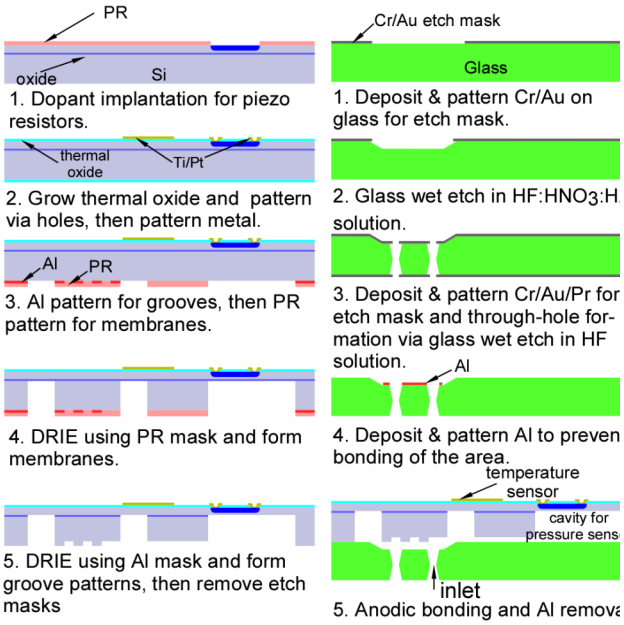

Fig. 3: Si-glass micromachining process: Sensors are formed on the device layer of the SOI wafer by various surface micromachining techniques. The buried oxide layer in SOI wafer acts as an etch stop for DRIE. A two step DRIE process is illustrated for SOI wafer. A glass wafer undergoes two wet etch process for a recess and through-hole formation. Then the two wafers are anodically bonded and diced.

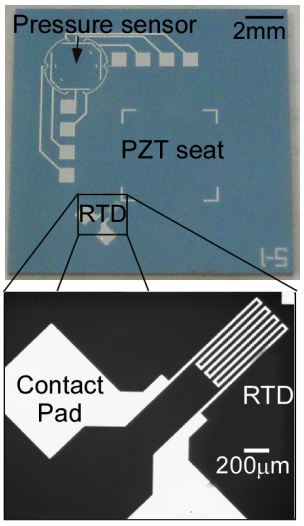

Fig. 4: Photograph of the metal contact layer with an expanded view of the platinum RTD.

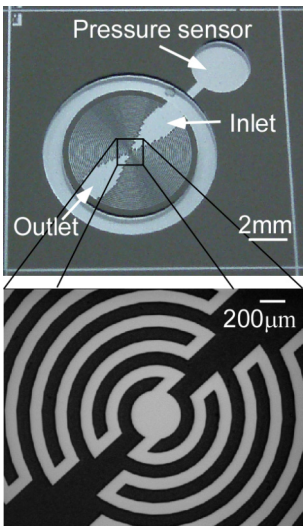

Fig. 5: Wide and expanded views of the circular serpentine groove patterns perimeter

400 μm deep. Next, the photoresist is removed and the Al is used as an etch mask for the final DRIE step, which engraves serpentine grooves for perimeter augmentation. The Al layer is then removed and the wafer is prepared for bonding. A processed silicon wafer die is shown in Figs. 4 and 5. Figure 4 shows the piezoresistive pressure sensor and platinum RTD with metal contact pads. Figure 5 shows the pressure sensor cavity and groove patterns for perimeter augmentation.

A recess of 2 μm is wet-etched into the glass wafer to accommodate the PZT displacement. Through holes are formed via HF wet etching. A thin layer of Al is deposited into the glass recess to prevent inadvertent bonding of the valve seat to the glass substrate due to the shallow recess depth. Anodic bonding is performed at 400°C and 800 V, after which the Al layer on the glass wafer is dissolved. The bonded wafers are then diced and prepared for assembly with the ceramic structure and PZT. The final step is to attach the PZT stack and ceramic cap using Stycast™ 2850 FT epoxy. To create a normally open valve, the PZT stack is energized during the assembly process so it shortens after assembly. The prototype valve structure is pictured in Fig. 6 attached to a ceramic header. The valve has dimensions of 1×1×1cm^3.

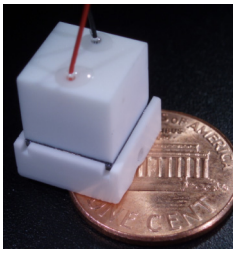

Fig. 6: Photograph of an assembled valve attached to a Macor header. The header is used to interface the valve with standardized tubing. It is pictured here with a US penny.

IV. EXPERIMENTAL AND MODELING RESULTS

Typical results obtained from a flexure type suspension valve are described in Figs. 7-11. In room temperature tests, the inlet pressure was regulated (21-55 kPa), and the outlet was maintained at atmosphere, while the flow rate was measured over 0-60 V actuation. As shown in Fig. 7, as actuation voltage increases, the PZT expands, the clearance between silicon valve seat and glass substrate decreases, and thus flow rate decreases. With 55 kPa of inlet pressure, flow rate was modulated from 0 to 980 mL/min. At 60 V, the valve leakage was below the measurement limit (< 0.1 mL/min.). These test results were compared with predicted values from a numerical flow model (Fig. 8). The model used a combination of reduced Navier Stokes 2-d equations and empirical formulations [1].

In a separate experiment, a pressure drop across the valve was recorded along with the flow rate as the actuation voltage was varied from 0 to 120 V (Fig. 9). At 145 kPa inlet pressure, a 28 kPa pressure drop across the valve was obtained by partially closing the exit valve, and a flow rate of 950 mL/min. was recorded. As the actuation voltage was increased, the valve restricted more flow while sustaining a larger pressure drop. At 120 V, it sustained a pressure drop of 130 kPa.

To verify the operations of the valve at cryogenic temperatures, another set of experiments were performed near the temperature of liquid nitrogen (80 K). The He gas was cooled by passing it through a liquid nitrogen heat exchanger. Inlet and outlet pressures were monitored. In addition, thermocouples were used to probe inlet and outlet gas temperature. The gas was then passed through another heat exchanger to bring it back to room temperature and exhausted to atmosphere, while the flow rate was measured. The valve performance is shown in Fig. 10 for inlet

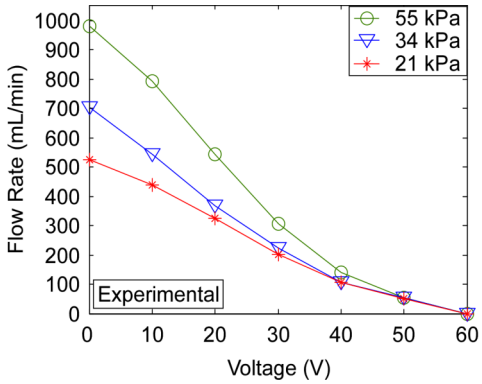

Fig. 7: Flow rates as a function of voltage at room temperature. As the actuation voltage increases, the valve is closed, which results in a decrease in flow rate.

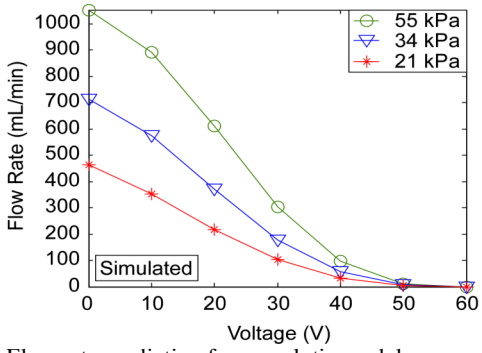

Fig. 8: Flow rate prediction from analytic model.

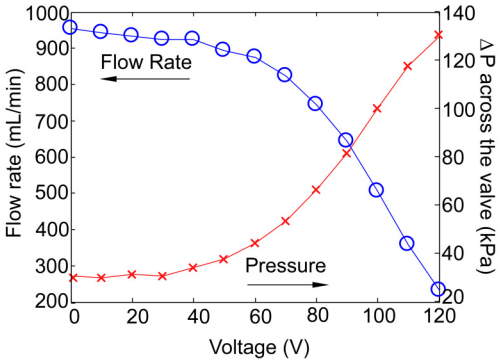

Fig. 9: Flow rate and inlet to outlet pressure differential as the valve with an inlet pressure of 145 kPa goes from the neutral position (0 V) to completely closed (120 V).

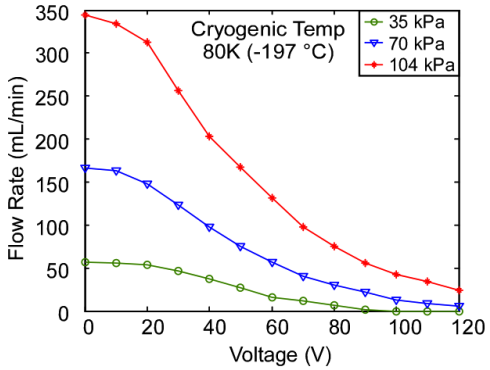

Fig. 10: Flow rates as a function of voltage at cryogenic temperature.

pressures 35 kPa, 70 kPa, and 104 kPa. Compared to the room temperature results, higher voltages were needed to completely close the valve. This is likely the result of the degraded piezoelectric coefficient at cryogenic temperatures [6].

Higher temperature flow tests were conducted at 107 ˚C to demonstrate a wide operating range. High temperature test results show similar modulation to previous tests. However, they require higher actuation voltages to fully close (Fig. 11). In addition, similar pressures resulted in higher flow rates in the high temperature tests than in the room temperature tests. We believe these effects are due to thermal expansion mismatch between the PZT and Macor that resulted in an increased gap at higher temperature.

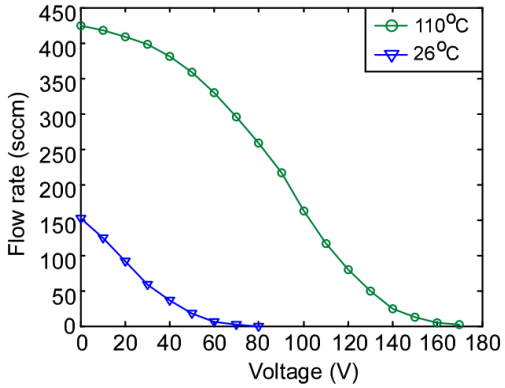

Fig. 11: Flow rates as a function of voltage at 110˚C and 26˚C with inlet pressure of 25 kPa.

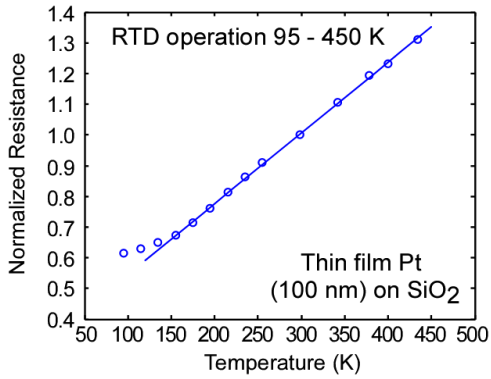

Fig. 12: Fractional change in RTD resistance versus temperature change. Baseline resistance was typically 490-510 ohms. Effective operating range is 150 – 450K, shown with a linear fit.

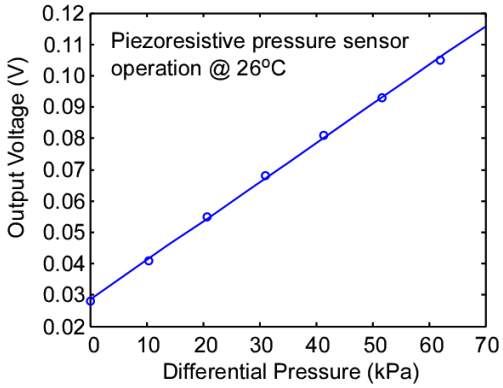

Fig. 13: Output voltage from the pressure sensor versus differential pressure shown with a linear fit.

Preliminary tests for the sensors that are being embedded with the valves were conducted. The resistance of the platinum RTD was measured across a temperature range from 95 to 450 K and the normalized resistances, referenced to room temperature resistance (≈500 Ω), are plotted in Fig. 12. The sensor showed sensitivity of 0.23%/K in its linear range of 150-450 K.

The pressure sensor was tested at room temperature. The Wheatstone bridge configuration in the piezoresistive pressure sensor was driven with 1 kHz, 5 V input and the output voltage amplitude was measured and plotted in Fig. 13 with a linear fit. The results demonstrate the linear characteristic of piezoresistive pressure sensors. Sensitivity was measured to be 250 ppm/kPa (33.3 ppm/Torr).

V. CONCLUSIONS

This effort has resulted in the successful fabrication of a piezoelectrically actuated ceramic-Si-glass microvalve for distributed cooling application. A perimeter augmentation scheme was used to overcome limited displacement of PZT and provide large flow modulation. Successful flow modulation was achieved across temperatures ranging from 80-380 K. Embedded sensors demonstrated good parameter sensitivity across large portions of this range.

ACKNOWLEDGMENTS

The authors are grateful to the Michigan Nanofabrication Facility at the University of Michigan. The authors also appreciate the contribution of Daniel Hoch at the University of Wisconsin in valuable discussions. This work is supported primarily by NASA under award NNA05CP85G.

REFERENCES

[1] J.M. Park, R.P. Taylor, A.T. Evans, T.R. Brosten, G.F. Nellis, S.A. Klein, J.R. Feller, L. Salerno, Y.B. Gianchandani, "A Piezoelectrically Actuated Ceramic-Si-Glass Microvalve for Distributed Cooling Systems," *Solid-State Sensor and Actuator Workshop,* Hilton Head Island, pp. 248-251, 2006

[2] I. Chakraborty, W.C. Tang, D.P. Bame, T.K. Tang, "MEMS Micro-valve for Space Applications," *Sensors and Actuators*, V. 83, pp. 188-193, 2000

[3] M. Esashi, S. Shoji, A. Nakano, "Normally Closed Microvalve and Micropump Fabricated on a Silicon Wafer," *Sensors and Actutors*, V. 20, pp. 163-169, 1989

[4] S. Shoji, B. Schoot, N. Rooij, M. Esashi, "Smallest Dead Volume Microvalves for Integrated Chemical Analyzing Systems," *Transducers '91*, pp. 1052-1055, 1991

[5] C. Lee, E.H. Yang, "A Piezoelectric Liquid-Compatible Microvalve for Integrated Micropropulsion," *Technical Digest of the 2004 Solid-State Sensor and Actuator Workshop*, Hilton Head Isl., SC, 6/6-10/04, pp. 160-163, 2004

[6] R.P. Taylor, et al., "Measurements of the Material Properties of a Laminated Piezoelectric Stack at Cryogenic Temperatures," *Conference Proceedings of the 2005 International Cryogenic Materials Conference*, v. 824, pp. 200-7, 2006